Chapter 19 - **THE SMEARING EFFECT**

In analyzing SANS data, smearing of the model function used is necessary before performing nonlinear least-squares fits. The smearing procedure involves a convolution integral between the resolution function and the scattering cross section for the scattering model.

1. THE RESOLUTION FUNCTION

Consider a 1D Gaussian resolution function (Barker-Pedersen, 1995):

$$P_{1D}(Q_x) = \left(\frac{1}{2\pi\sigma_{Q_x}^{\,2}}\right)^{1/2} \exp\left[-\frac{Q_x^{\,2}}{2\sigma_{Q_x}^{\,2}}\right] \qquad (1)$$

This distribution is normalized to 1. $\int_{-\infty}^{+\infty} dQ_x P_{1D}(Q_x) = 1$.

In order to show this normalization, make a variable change to $X = Q_x^{\,2}$ so that $dX = 2Q_x dQ_x$ and the normalization integral becomes as follows.

$$\int_{-\infty}^{+\infty} dQ_x P_{1D}(Q_x) = 2\int_{0}^{+\infty} dQ_x P_{1D}(Q_x) = 2\int_{0}^{+\infty} dX \frac{1}{2\sqrt{X}} \left(\frac{1}{2\pi\sigma_{Q_x}^{\,2}}\right)^{1/2} \exp\left[-\frac{X}{2\sigma_{Q_x}^{\,2}}\right]. \qquad (2)$$

The following integral is used:

$$\int_{0}^{+\infty} dX \frac{1}{\sqrt{X}} \exp[-aX] = \sqrt{\frac{\pi}{a}} \quad \text{(for a>0)} \qquad (3)$$

This verifies that the $P_{1D}(Q_x)$ distribution is normalized. The Q_y distribution is similar.

Consider a 2D Gaussian resolution function:

$$P_{2D}(Q) = P_{1D}(Q_x)P_{1D}(Q_y) \qquad (4)$$

$$= \left(\frac{1}{2\pi\sigma_{Q_x}^{\,2}}\right)^{\frac{1}{2}} \left(\frac{1}{2\pi\sigma_{Q_y}^{\,2}}\right)^{\frac{1}{2}} \exp\left[-\frac{Q_x^{\,2}}{2\sigma_{Q_x}^{\,2}} - \frac{Q_y^{\,2}}{2\sigma_{Q_y}^{\,2}}\right].$$

This distribution is also normalized to 1.

$$\int_0^{+\infty} QdQ \int_0^{2\pi} d\phi P_{2D}(Q) = 1 \qquad (5)$$

In order to show this, make a variable change to $R = Q^2$ and $dR = 2QdQ$ so that the normalization integral becomes as follows.

$$\int_0^{+\infty} QdQ \int_0^{2\pi} d\phi P_{2D}(Q) = \frac{1}{2} \int_0^{+\infty} dR \left(\frac{1}{\pi \sigma_Q^{\,2}} \right) \exp\left[\frac{-R}{\sigma_Q^{\,2}} \right] (2\pi) = \left[-\exp\left(-\frac{\infty}{\sigma_Q^{\,2}} \right) + \exp\left(-\frac{0}{\sigma_Q^{\,2}} \right) \right] = 1. \qquad (6)$$

2. THE RESOLUTION CORRECTION

The smeared 1D cross section corresponds to radially averaged SANS data and is given by the following integral (using polar coordinates):

$$\left[\frac{d\Sigma(Q)}{d\Omega} \right]_{\text{smeared}} = \int_0^{+\infty} dQ' P_{1D}(Q') \frac{d\Sigma(Q - Q')}{d\Omega} =$$

$$= \int_0^{+\infty} dQ' \left(\frac{1}{2\pi \sigma_{Q'}^{\,2}} \right)^{1/2} \exp\left[-\frac{Q'^2}{2\sigma_{Q'}^{\,2}} \right] \frac{d\Sigma(Q - Q')}{d\Omega}. \qquad (7)$$

The smeared 2D cross section integral corresponds to 2D SANS data and is given by the following expression:

$$\frac{d\Sigma(Q_x, Q_y)}{d\Omega} = \int_{-\infty}^{+\infty} dQ'_x \, P_{1D}(Q'_x) \int_{-\infty}^{+\infty} dQ'_y \, P_{1D}(Q'_y) \frac{d\Sigma(Q_x - Q'_x, Q_y - Q'_y)}{d\Omega} \qquad (8)$$

Note that (Q_x,Q_y) are in Cartesian coordinates. In cases where radial averaging of the data is not possible, the $\sigma_{Qx}^{\,2}$ and $\sigma_{Qy}^{\,2}$ variances are needed. Note that the variance $\sigma_Q^{\,2} = \sigma_{Qx}^{\,2} + \sigma_{Qy}^{\,2}$ is never used.

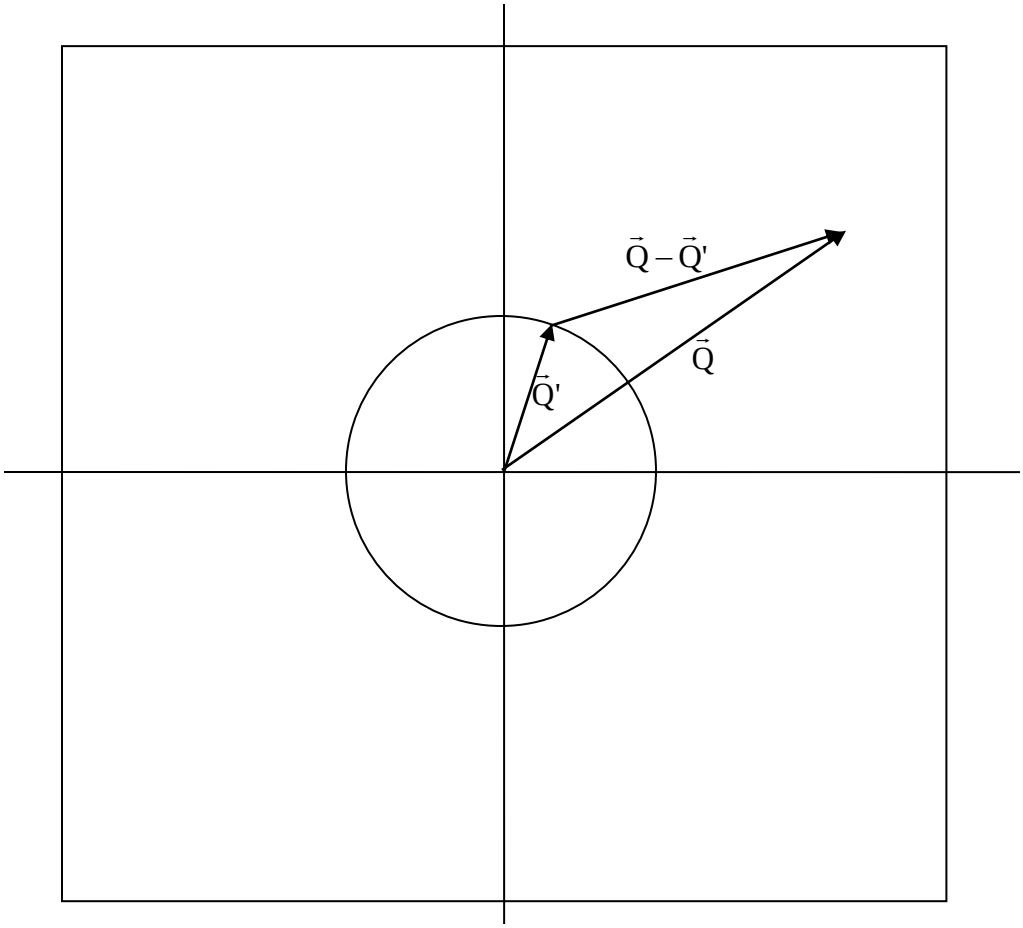

Figure 1: Parametrization in the detector plane.

3. ISO-INTENSITY CONTOUR MAPS WITH GRAVITY EFFECT

Gravity effect on the neutron trajectory distorts the iso-intensity contour maps from concentric circles to concentric oval shapes. The following parametric equation describes an elliptical shape:

$$\frac{x^2}{a^2}+\frac{y^2}{(a+b)^2}=1. \qquad (9)$$

Here a is the minor (horizontal) axis and a+b is the major (vertical) axis of the elliptical shape. If we consider different major axes for the top and bottom parts, an oval shape is obtained.

$$b = A(2\bar{\lambda}\Delta\lambda - \mathrm{sign}(y)\Delta\lambda^2). \qquad (10)$$

The top and bottom parts have been represented using the sign function. The x and y coordinates can be expressed as:

$$x = r(\phi)\cos(\phi) \qquad (11)$$
$$y = r(\phi)\sin(\phi)\,.$$

ϕ is the azimuthal angle for binning in the detector plane. Combining these equations, one obtains the following parametric equation:

$$r^2(\phi) = \frac{1}{\frac{\cos^2\phi}{a^2} + \frac{\sin^2\phi}{(a+b)^2}}\,. \qquad (12)$$

Note that this applies to Q = 0 only.

4. NUMERICAL APPLICATION

Consider the following realistic case:

$$L_1 = 16.14 \text{ m} \qquad (13)$$
$$L_2 = 13.19 \text{ m}$$
$$\bar{\lambda} = 18 \text{ Å}$$
$$\frac{\Delta\lambda}{\lambda} = 0.13$$
$$A = 0.01189 \text{ cm/Å}^2$$

This gives

$$\lambda_{min} = 15.66 \text{ Å}\,,\ \lambda_{max} = 20.34 \text{ Å}\,.$$

The following beam spot characteristics are obtained:

$$y_{min} = 2.916 \text{ cm}\,,\ y_{max} = 4.919 \text{ cm}$$
$$\bar{y} = 3.852 \text{ cm}\,,\ < y >= 3.863 \text{ cm}$$
$$\Delta y_{top} = y_{max} - \bar{y} = 1.0667 \text{ cm}$$
$$\Delta y_{bot} = \bar{y} - y_{min} = 0.9365 \text{ cm}$$

Here $\bar{y}$ is the spot height corresponding to the mean wavelength $\bar{\lambda}$ and $< y >$ is the vertical location of the beam center. Note that for any practical purpose $\bar{y} =< y >$ and the difference $\Delta y_{top} - \Delta y_{bot} = 0.130 \text{ cm}$ is so small that the oval shapes are really elliptical.

The beam standard deviation in the vertical direction is estimated to be $\sigma_y = 0.409\,\text{cm}$ using both the numerical integration over y and the analytical averaging over λ (formula given above).

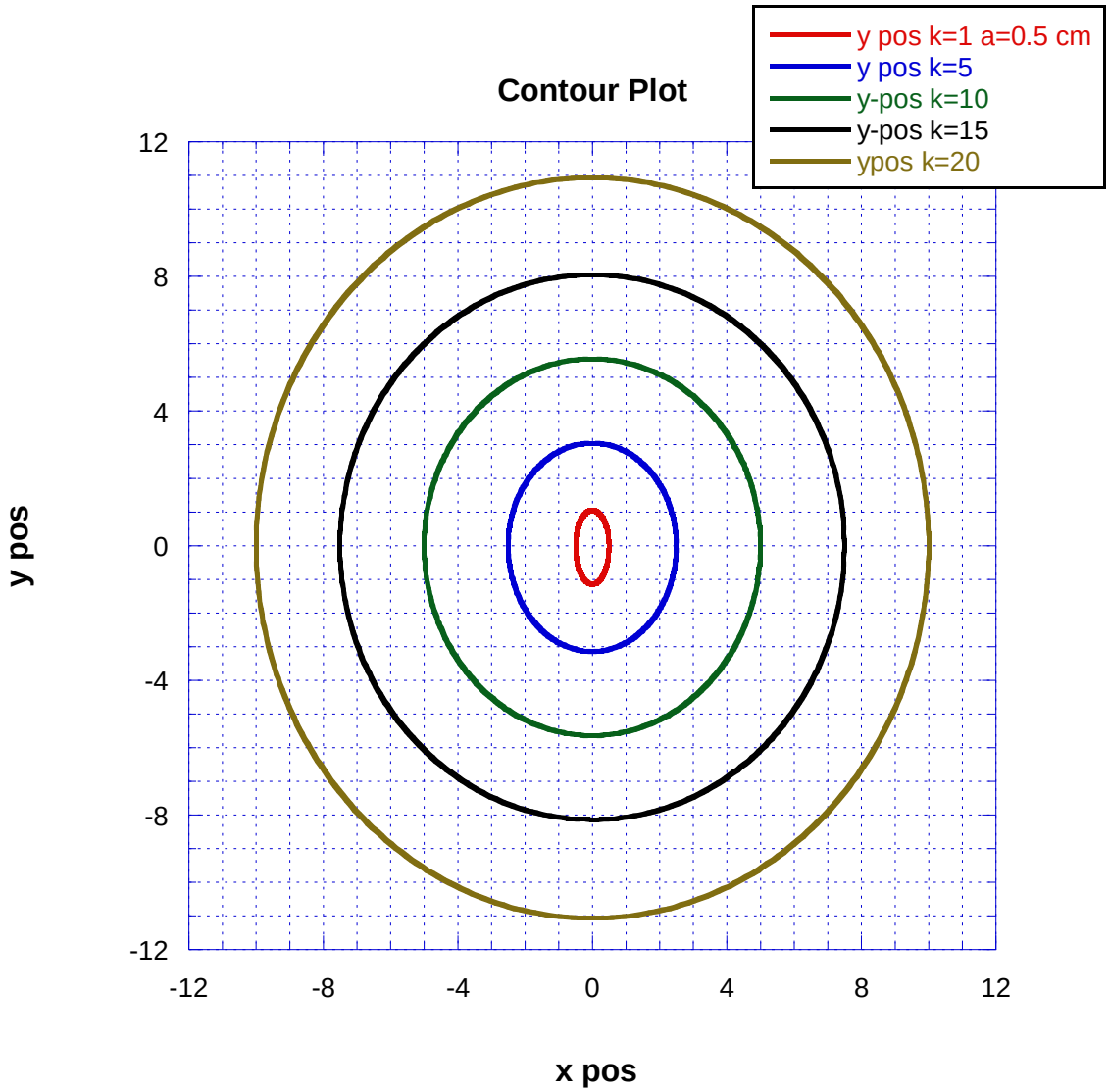

Figure 2: Iso-intensity contour map when neutrons are under the influence of gravity; i.e., at long wavelength (λ = 18 Å) and typical wavelength spread ($\Delta\lambda/\lambda = 13\%$). Contours corresponding to a = 0.5 cm and k = 1, 5, 10, 15 and 20 are shown. The x and y axes are in channel numbers (each detector channel corresponds to 0.5 cm).

5. SMEARING FOR HARD SPHERES

Consider idealized scattering from hard spheres and compare it to the smeared case. The form factor for a hard sphere of radius R = 50 Å is given by the following function:

$$P(Q) = \left[\left(\frac{3}{QR} \right) \left(\frac{\sin(QR)}{(QR)^2} - \frac{\cos(QR)}{QR} \right) \right]^2 \qquad (14)$$

Consider the following high-Q configuration:

$$\begin{aligned} &R_1 = 2.5 \text{ cm} \\ &R_2 = 0.5 \text{ cm} \\ &\Delta x_3 = \Delta y_3 = 0.5 \text{ cm} \\ &L_1 = 1.5 \text{ m} \\ &L_2 = 1.5 \text{ m} \\ &\lambda = 6 \text{ Å} \\ &\frac{\Delta\lambda}{\lambda} = 15\ \%. \end{aligned} \qquad (15)$$

The direct beam spatial resolution on the detector plane is:

$$\begin{aligned} &\sigma_x^2 = 1.83 \text{ cm}^2 \\ &\sigma_y^2 = 1.83 \text{ cm}^2. \end{aligned} \qquad (16)$$

The variance of the Q resolution is:

$$\begin{aligned} &\sigma_{Qx}^{\ 2} = 8.94 * 10^{-5} + 0.0037\, Q_x^{\ 2} \text{ (in units of Å}^{-2}) \\ &\sigma_{Qy}^{\ 2} = 8.94 * 10^{-5} + 0.0037\, Q_y^{\ 2} \text{ (in units of Å}^{-2}). \end{aligned} \qquad (17)$$

The wavelength spread contribution dominates for this high-Q configuration. The gravity contribution is negligible for the 6 Å wavelength.

For this high-Q configuration,

$$Q_{min}^{X} = Q_{min}^{Y} = 0.028 \text{ Å}^{-1}. \qquad (18)$$

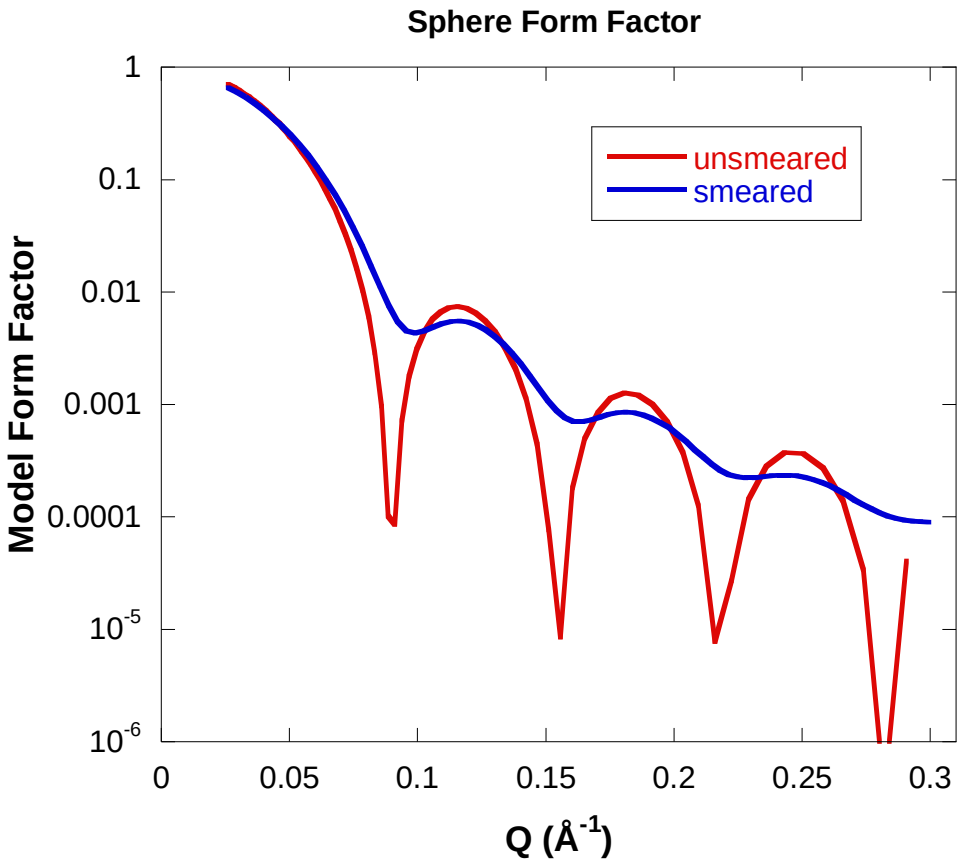

Figure 3: Plot of the form factor for a sphere of radius R = 50 Å before and after smearing produced by the high-Q configuration.

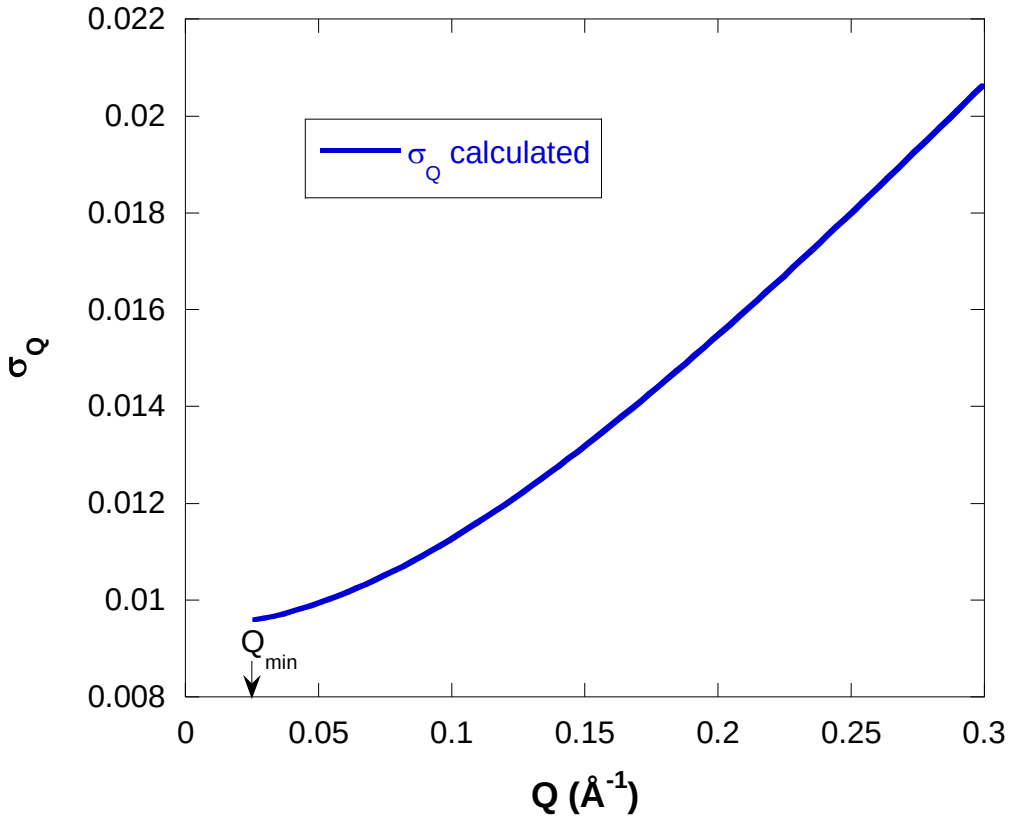

Figure 4: Variation of the standard deviation of the Q resolution *vs* Q.

Consider the following low-Q instrument configuration and spheres of radius R = 500 Å.

$$R_1 = 2.5 \text{ cm} \quad (19)$$
$$R_2 = 0.5 \text{ cm}$$
$$\Delta x_3 = \Delta y_3 = 0.5 \text{ cm}$$
$$L_1 = 15 \text{ m}$$
$$L_2 = 15 \text{ m}$$
$$\lambda = 12 \text{ Å}$$
$$\frac{\Delta\lambda}{\lambda} = 15\ \%.$$

Therefore:

$$A = 0.0138 \text{ cm/Å}^2 \quad (20)$$
$$\sigma_x^2 = 1.83 \text{ cm}^2$$
$$\sigma_y^2 = 1.83 \text{ cm}^2$$

So that:

$$\sigma_{Qx}^{\ 2} = 2.23*10^{-7} + 0.0037\, Q_x^{\ 2} \text{ (in units of Å}^{-2}\text{)} \quad (21)$$

$$\sigma_{Qx}^{\ 2} = 2.31*10^{-7} + 0.0037\, Q_y^{\ 2} \text{ (in units of Å}^{-2}\text{)}.$$

The first term is slightly different for σ_{Qx} and σ_{Qy} because of the small gravity contribution. For this configuration, the geometry part dominates at low-Q, the wavelength-spread part contributes at higher Q, and the gravity term is small.

For this low-Q configuration,

$$Q_{min}^{X} = 0.0014 \text{ Å}^{-1}, \qquad (22)$$
$$Q_{min}^{Y} = 0.0016 \text{ Å}^{-1}.$$

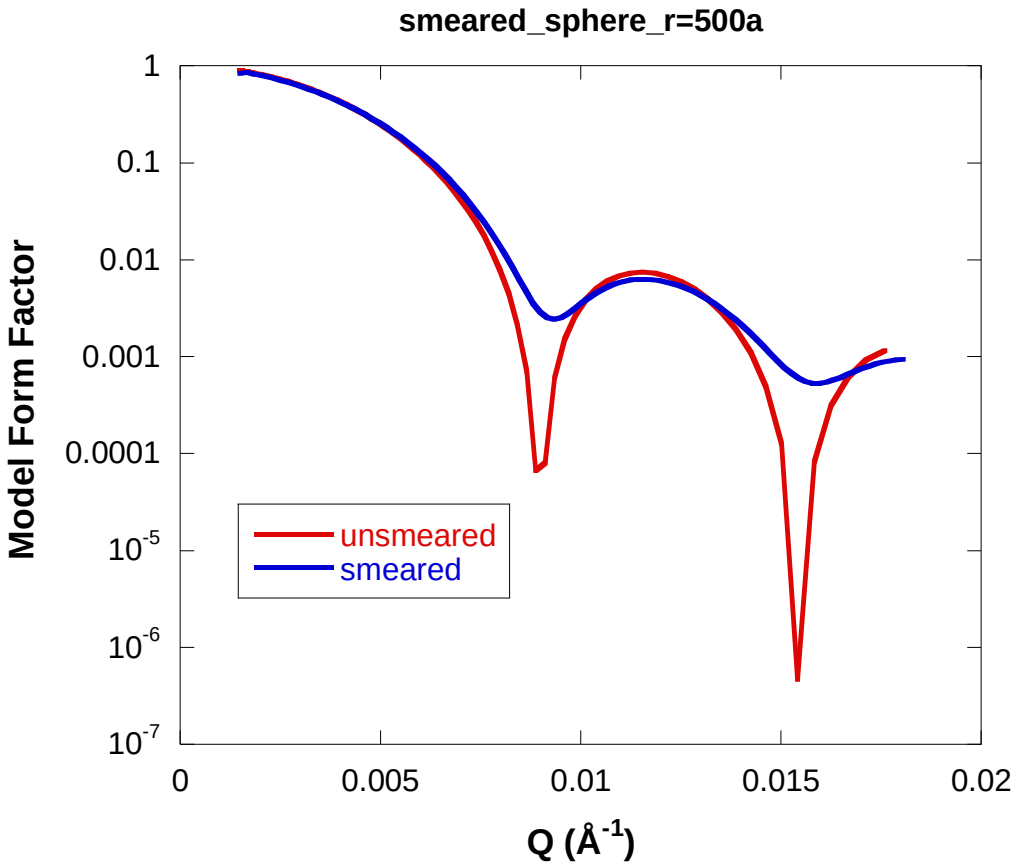

Figure 5: Plot of the form factor for a sphere of radius R = 500 Å before and after smearing produced by the low-Q configuration.

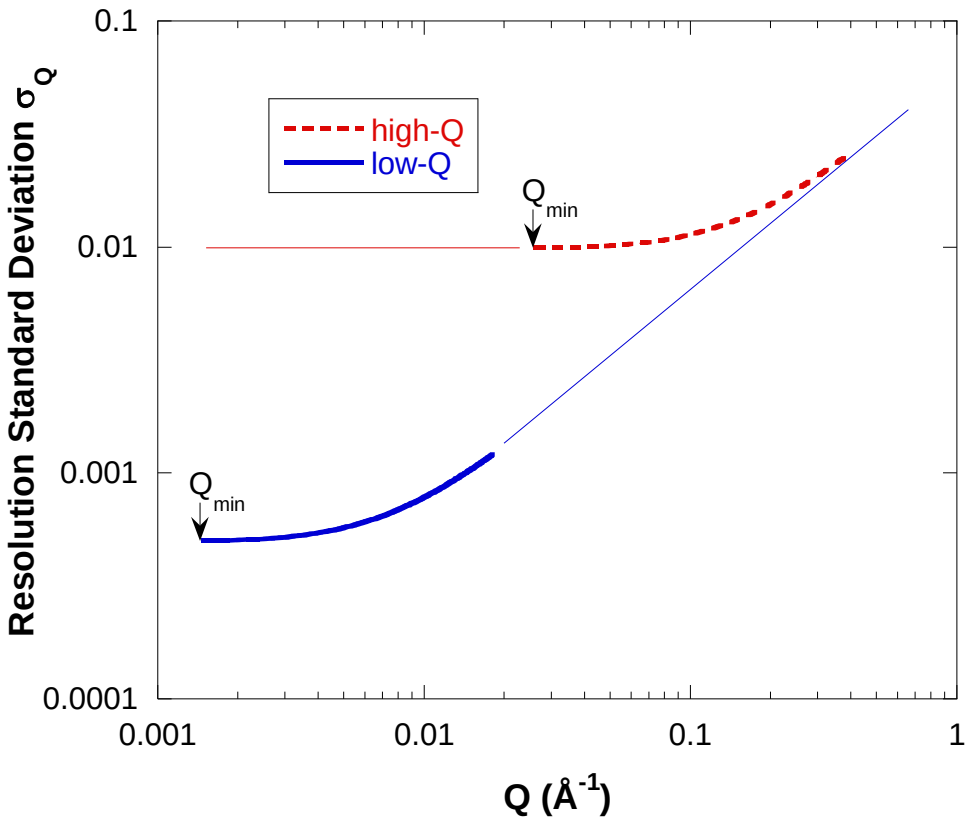

Figure 6: Plot of the standard deviation of the Q resolution for both the low-Q and the high-Q configurations. The values of Q_{min} are also indicated.

6. SANS FROM SILICA PARTICLES

SANS data have been taken from a dilute solution of monodisperse silica particles in D_2O (volume fraction of 0.1 %) and fit to the sphere model. Fit results gave a sphere radius of R = 563.51 ± 0.45 Å. SANS data were taken using a low-Q instrument configuration.

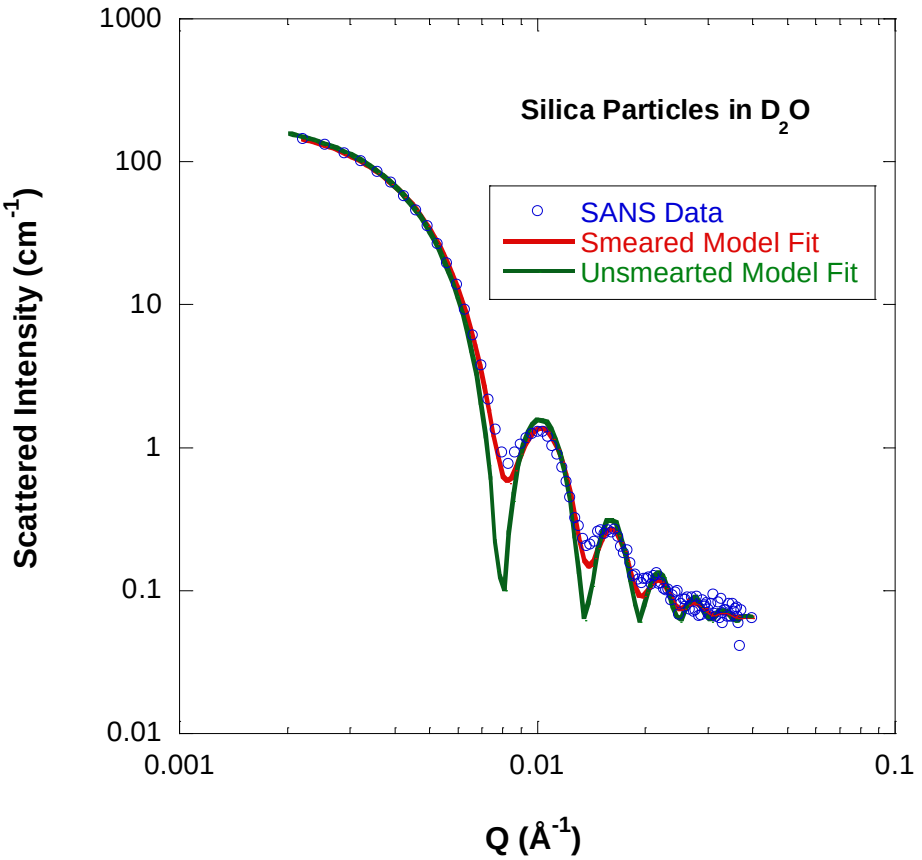

Figure 7: SANS data from a dilute solution of monodisperse silica particles in D_2O along with the fit to the sphere model.

REFERENCE

J.G. Barker, and J.S. Pedersen, "Instrumental Smearing Effects in Radially Symmetric SANS by Numerical and Analytical Methods", J. Appl. Cryst. 28, 105-114 (1995).

QUESTIONS

1. What are the two ways of accounting for instrumental resolution?
2. Is it OK to perform a 1D smearing convolution integral on 2D SANS data?
3. What is the effect of instrumental smearing on the radius of gyration obtained from a Guinier fit?
4. What are the two ways of correcting for the effect of gravity?

ANSWERS

1. Instrumental resolution is included either (1) by smearing of the model used to fit the data or (2) by desmearing the data through an iterative process. Method (1) is the most reliable and the most used. Method (2) does not work well when sharp peaks appear in the data.
2. It is OK to perform a 1D smearing convolution integral if the 2D SANS data are azimuthally symmetric (scattering is isotropic).
3. Instrumental resolution tends to broaden peaks. The Guinier region is the tail of a peak at Q = 0. Broadening implies a lower slope and therefore a lower radius of gyration. The smeared radius of gyration is lower than the real value.
4. Gravity correction can be made (1) through a software method by defining constant-Q elliptical bins or (2) through a hardware method using gravity-correcting prisms.